

Radiation hard polyimide-coated FBG optical sensors for relative humidity monitoring in the CMS experiment at CERN

This content has been downloaded from IOPscience. Please scroll down to see the full text.

2014 JINST 9 C03040

(<http://iopscience.iop.org/1748-0221/9/03/C03040>)

View [the table of contents for this issue](#), or go to the [journal homepage](#) for more

Download details:

IP Address: 219.90.92.90

This content was downloaded on 05/12/2015 at 06:59

Please note that [terms and conditions apply](#).

RECEIVED: November 29, 2013

REVISED: January 9, 2014

ACCEPTED: January 22, 2014

PUBLISHED: March 24, 2014

13th TOPICAL SEMINAR ON INNOVATIVE PARTICLE AND RADIATION DETECTORS
7–10 OCTOBER 2013
SIENA, ITALY

Radiation hard polyimide-coated FBG optical sensors for relative humidity monitoring in the CMS experiment at CERN

A. Makovec,^{a,1} G. Berruti,^{b,d} M. Consales,^b M. Giordano,^c P. Petagna,^d
S. Buontempo,^{e,d} G. Breglio,^f Z. Szillasi,^{g,d} N. Beni^{g,d} and A. Cusano^b

^aUniversity of Debrecen,
HU-4032 Debrecen, Hungary

^bOptoelectronic Division – Engineering Department, University of Sannio,
I-82100 Benevento, Italy

^cIMCB – National Research Council,
I80055 Portici, Italy

^dPH Department, DT Section, CERN – European Organization for Nuclear Research,
CH-1211 Geneva, Switzerland

^eINFN – Istituto Nazionale di Fisica Nucleare,
I 80126 Napoli, Italy

^fDepartment of Electrical Engineering and Information Technology,
I-80138 Napoli, Italy

^gAtomki – Institute for Nuclear Research, Hungarian Academy of Sciences,
H-4026 Debrecen, Hungary

E-mail: AlajosMakovec@cern.ch

ABSTRACT: This work investigates the performance and the radiation hardness capability of optical thermo-hygrometers based on Fibre Bragg Gratings (FBG) for humidity monitoring in the Compact Muon Solenoid (CMS), one of the four experiments running at CERN in Geneva. A thorough campaign of characterization was performed on 80 specially produced Polyimide-coated RH FBG sensors and 80 commercial temperature FBG sensors. Sensitivity, repeatability and accuracy were studied on the whole batch, putting in evidence the limits of the sensors, but also showing that they can be used in very dry conditions. In order to extract the humidity measurements from the sensor readings, commercial temperature FBG sensors were characterized in the range of interest.

¹Corresponding author.

Irradiation campaigns with ionizing radiation (γ -rays from a Co^{60} source) at incremental absorbed doses (up to 210 kGy for the T sensors and up to 90 kGy for the RH sensors) were performed on sample of T and RH-Sensors. The results show that the sensitivity of the sensors is unchanged up to the level attained of the absorbed dose, while the natural wavelength peak of each sensor exhibits a radiation-induced shift (signal offset). The saturation properties of this shift are discussed.

KEYWORDS: Detector design and construction technologies and materials; Interaction of radiation with matter; Detector cooling and thermo-stabilization

Contents

1	Introduction	1
2	Fiber Bragg grating sensors for relative humidity measurement	2
2.1	Sensing principle	2
2.2	FOS thermo-hygrometer based on FBG technology	3
3	Experimental set-up	3
4	Characterisation of FOS thermo-hygrometer	4
4.1	FBG temperature sensors	4
4.2	FBG relative humidity sensor	5
4.2.1	Linear model	5
4.2.2	Surface model	6
5	Radiation hardness study	7
5.1	Radiation hardness of the FOS temperature sensors	7
5.2	Radiation hardness of the FOS relative humidity sensors	8
6	Conclusions	10

1 Introduction

In the core of the Compact Muon Solenoid (CMS) experiment — one of the four large experiments of the LHC experiment at CERN — the Silicon Tracker measures momentum and position of the charged particles with more than 16000 silicon micro-strip and pixel sensors. However, the high radiation level resulting from the operation of LHC at full luminosity can cause serious deterioration of their performance. To increase their lifetime, the silicon sensors in the Tracking detectors at LHC must be kept cold. At the restart of LHC after the First Long Shut-down phase, the CMS Tracker will operate under the constraint that the warmest point on the surface of each silicon sensor is kept at a temperature below -10°C . In order to reach this condition, the temperature of the fluids cooling the CMS Tracker sub-detectors will be progressively lowered to values between -20°C and -30°C .

Monitoring the ambient parameters, notably temperature and humidity, and avoid any condensation risk is vital for a safe exploitation of the detector, not only inside the Tracker, but also in the surrounding volume, where the pipes transporting the cold refrigerant are embedded in the service trays and distributed all around volume. In addition, tracking detectors need to be as much as possible transparent to particles and the space available in the surrounding volume for additional cables and sensors is extremely limited: this requires the minimization of the mass, size and required

services of all the devices to be integrated inside experiment. Furthermore, while the experiment is designed for an operational life in excess of 10 years, the possibilities of maintenance access to the area surrounding the Tracker are extremely limited, and those inside are virtually impossible. Last, but not least, any humidity sensor to be introduced in the detector volume should ideally comply with the requirement of radiation resistance to dose ranging from 10 kGray up to 1 MGray, and it must be also insensitive to magnetic field too.

In this scenario, fiber optic sensors (FOS) appear as a very good alternative to the conventional instruments used at the present. Indeed, the fiber itself can tolerate a very high level of radiation [1]; optical fiber transmission is insensitive to magnetic field and electromagnetic noise, and is perfectly suited for read-out over very long distances. Furthermore, the availability of multi-point sensing techniques based on Fiber Bragg Grating (FBG) allows for sensing on several tens of points along the same fiber, thus dramatically reducing the amount of services required for distributed measurements. While successful use of FBG sensor arrays for temperature and strain monitoring in CMS has been already previously reported [2], the possibility of using FBG in connection with moisture sensitive polymer coating as a mean of Relative Humidity (RH) detection has been also recently demonstrated [3, 4]. Further investigations performed at CERN on FBG sensors coated in-house under controlled conditions have demonstrated the strong potentialities of the proposed technology in terms of stable and repeatable measurements — also at very low temperature — and tolerance to radiations, up to 10 kGy [5]. Lately, other groups have recently suggested that a less controlled and more economic industrial production may be also suitable for RH monitoring in High Energy Physics experiments [6].

2 Fiber Bragg grating sensors for relative humidity measurement

2.1 Sensing principle

A FBG is a permanent periodic modulation of the refractive index in the core of a single-mode optical fiber. It behaves as a wavelength selective filter which reflects light signals at a specific wavelength, named the Bragg wavelength (λ_B), that is strictly dependent on the fiber effective refractive index (n_{eff}) and the grating pitch (Λ) of the FBG:

$$\lambda_B = 2n_{\text{eff}}\Lambda. \quad (2.1)$$

Both the refractive index and the grating pitch can be affected by strain and temperature [7].

An axial strain in the grating changes the grating spatial period, as well as the effective refractive index and results in a shift on the Bragg wavelength due to the elastic behaviour and the elasto-optic effect. On the other hand, the change of ambient temperature has a similar effect, due to the thermal expansion and the thermo-optic effect, (figure 1). The Bragg wavelength shift due to the change in strain (ε) and thermal effect (ΔT) can be expressed as [8]:

$$\Delta\lambda_B/\lambda_B = (1 - P_e)\varepsilon + [(1 - P_e)\alpha + \xi]\Delta T \quad (2.2)$$

where P_e is the photo elastic-constant of the fiber, α is the thermal-expansion coefficient and ξ is the thermo-optic coefficient of the fiber.

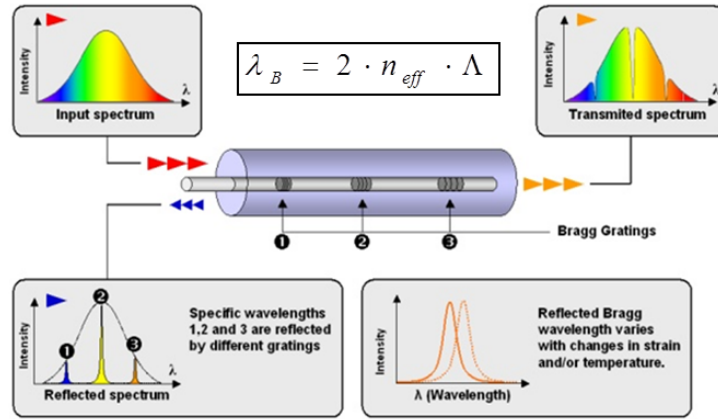


Figure 1. Sensing mechanism of the FBG sensors.

2.2 FOS thermo-hygrometer based on FBG technology

Bare silica fibers are insensitive to humidity. However, it is possible to use an FBG as humidity sensor by coating it with a hygroscopic material that swells as a consequence of water molecules adsorption. The swelling of the moisture sensitive coating strains the fiber, thus inducing a mechanical strain to the FBG that, in turn, results in a Bragg wavelength shift.

In presence of variations in RH (ΔRH) and T (ΔT), in the linear assumption, the Bragg wavelength shift can be expressed as [3, 8]:

$$\Delta \lambda_B = f(\Delta RH, \Delta T) = S_{RH} \Delta RH + S_T \Delta T \quad (2.3)$$

where S_{RH} and S_T are respectively the relative humidity sensitivity and temperature sensitivity. In the most general case, S_{RH} and S_T are functions of both temperature and humidity.

The S_{RH} of polyimide-coated FBGs, as well as their response time, is linked to the thickness of the coating material [8]. It is worth noting that, due to the FBG inherent sensitivity to temperature, a temperature compensation scheme is required to decouple the cross-sensitivity to strain and temperature and, thus, to extract RH measurements from the sensor readings. This can be simply accomplished by using an additional T-Sensor which must be located as close as possible to the RH-Sensor, as shown in figure 2. The solution proposed to CMS is an optical thermo-hygrometer made by two coupled FBGs, one polyimide coated and the other bare, for RH and T readings, respectively. However, due to the intrinsic characteristic of the mechanical action of the polyimide coating swelling under moisture absorption, the value of S_T referred to a 1°C variation is typically found to be one order of magnitude higher than the value of S_{RH} referred to a 1% RH variation [5]. A high precision temperature measurement is therefore essential to avoid large errors induced on the RH reading.

3 Experimental set-up

The characterization tests of the FOS sensors require a well-controlled environment. In order to satisfy this requirement, the tests were conducted in the PH-DT test facility at CERN. The climatic chamber is provided with a thermo-regulation circuit for temperature control, while a

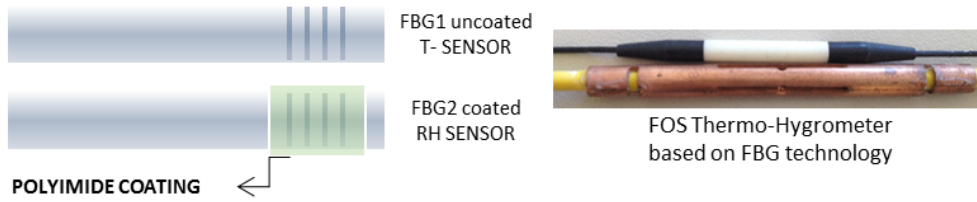


Figure 2. FOS thermo-hygrometer based on FBG sensors.

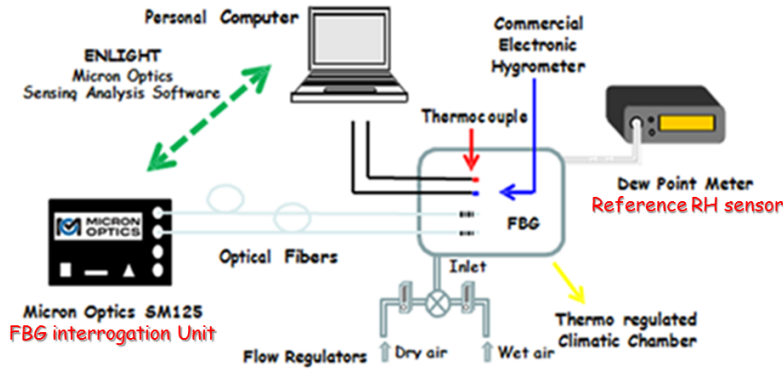


Figure 3. Experimental Set-Up.

precise control of the relative humidity is ensured manually, using a system of valves. The tests cover the range of ambient RH [0 to 90] % in the temperature range [−20 to +30]°C. A schematic illustration of the set-up is shown in figure 3.

The FBG FOS Sensors were installed in the chamber and interrogated by a state-of-the-art Optical Interrogator (Micron Optic sm125) with 1 pm wavelength resolution. As a reference sensor, a high performance Chilled Mirror Dew Point Hygrometer was used for measuring the RH. As reference temperature sensors, calibrated resistance thermometers (PT-100) were placed close to the FBGs.

4 Characterisation of FOS thermo-hygrometer

4.1 FBG temperature sensors

Since a polyimide coated FBG sensor is sensitive to T variation, temperature compensation is vital. The selected Micron Optic commercial FBG sensors (os4300) were fully characterized in the range of interest in order to achieve a very precise T monitoring. Temperature calibration cycles were performed for all the 80 FOS T-Sensors between −20 and 20°C with 5°C steps.

Figure 4 shows the measurement accuracy of 8 samples after calibration using a cubic fitting curve:

$$T = a(\lambda + \lambda_{os})^3 + b(\lambda + \lambda_{os})^2 + c(\lambda + \lambda_{os}) + d \quad (4.1)$$

where a , b , c and d are the fitting parameters, T is temperature, λ and λ_{os} are the measured wavelength value and the offset parameter, respectively. All the tested FOS temperature sensors show

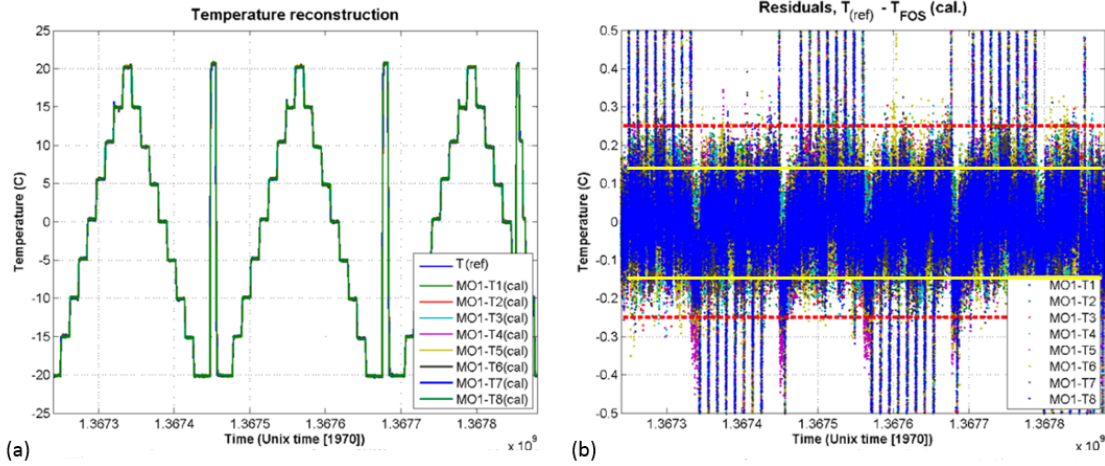


Figure 4. Reconstructed temperature values (a) measured by eight Temperature FBGs. Residuals are inside $\pm 0.15^\circ\text{C}$ at steady states (b).

good results in terms of stability, repeatability and accuracy: the residuals, evaluated as the difference between T_{FOS} and T_{Ref} , are reported in figure 4b for a sample of eight sensors. Despite the different dynamics of the FOS and the reference sensors, the residuals are all inside $\pm 0.15^\circ\text{C}$ in steady states.

4.2 FBG relative humidity sensor

The relative humidity FOS Sensors were produced under specification by an external company with a polyimide coating of 10 microns ($\pm 2 \mu\text{m}$) [5]. In order to take into account the double dependency of the sensor on the swelling of the coating material in presence of moisture on one hand, and on the sensitivity of the grating to temperature variations on the other hand, two models were applied: a linear model and a higher order surface model.

4.2.1 Linear model

This method is described in the literature and based on the mathematical model which describes the absorption or desorption phenomena of water molecules into the coating of the grating in a linear approximation, according to eq. (2.3).

RH tests were performed in the range $[0 - 50] \%$ at four different temperatures — namely $[20, 10, 0, -5]^\circ\text{C}$, (figure 5a).

The observed S_{RH} and S_{T} values are in a good agreement with the data found in the literature: $S_{\text{RH,mean}} = 1.39 \pm 0.07 \text{ pm}/\% \text{RH}$ and $S_{\text{T,mean}} = 11.30 \pm 0.11 \text{ pm}/^\circ\text{C}$. As anticipated, S_{T} is one order of magnitude higher than S_{RH} . However, as shown in figure 5b, 5c, cross-sensitivities to T and RH were also observed. Equation (2.3) can be expressed as follows:

$$\Delta\lambda_B = S_{\text{RH}}(T)\Delta\text{RH} + S_{\text{T}}(\text{RH})\Delta T. \quad (4.2)$$

A simplified linear approach cannot take into account this higher order dependence.

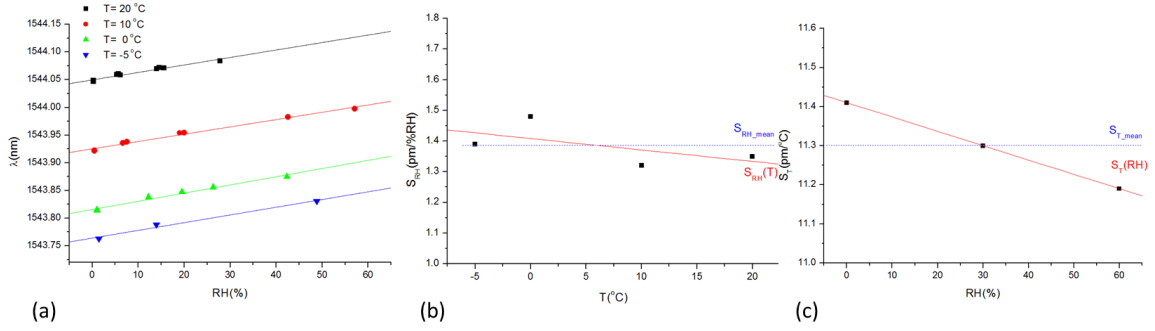


Figure 5. Calibration points measured at four different temperatures (a). S_{RH} as a function of Temperature (b) and S_T as a function of Relative Humidity (c).

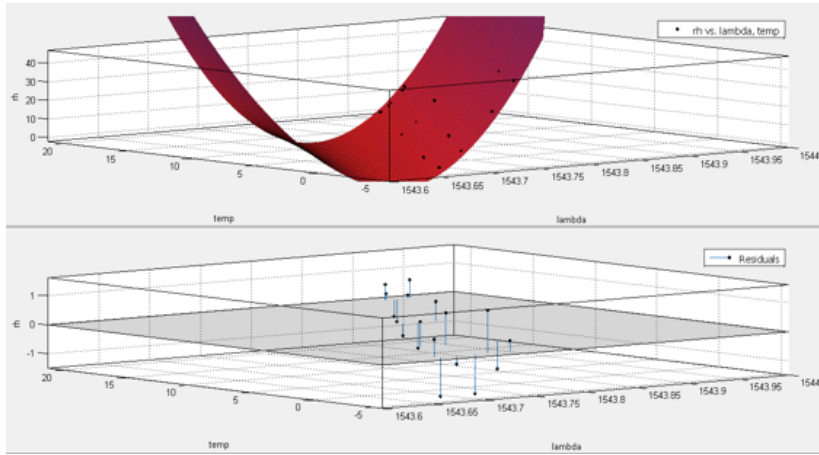


Figure 6. Sample calibration surface with fitting errors.

4.2.2 Surface model

In order to be able to describe the above mentioned cross-sensitivities to temperature and relative humidity, a higher order method (surface model) was introduced. Several daylong RH cycles were performed by cycling the temperature between -20 and 20°C , with 5°C steps, allowing RH changes in the chamber in the range $[0-50]\%$. As the measured wavelength value — given by a FOS RH-Sensor — is a function of the current relative humidity and temperature values, the measured RH can be expressed as:

$$RH(\lambda, T) = p_{00} + p_{10}\lambda + p_{01}T + p_{20}\lambda^2 + p_{11}\lambda T + p_{02}T^2 \quad (4.3)$$

where p_{00} , p_{10} , p_{01} , p_{20} , p_{11} and p_{02} are parameters. The term λT is introduced in order to point out the correlation between the wavelength and the T . Equation (4.3) describes a surface which can be used as calibration surface fitting the measured $RH(\lambda, T)$ values, where the fit provides the above mentioned parameters. An example of calibration surface is shown in figure 6.

For calibration, data from several daylong cycles were used. Different tests were also performed in order to produce independent data for the reconstructions. Figure 7 shows the performances of four samples of FOS Thermo-Hygrometers: the residuals, evaluated as the difference between RH_{FOS} and RH_{Ref} (Chilled Mirror), are inside $\pm 2\%$ RH in steady states.

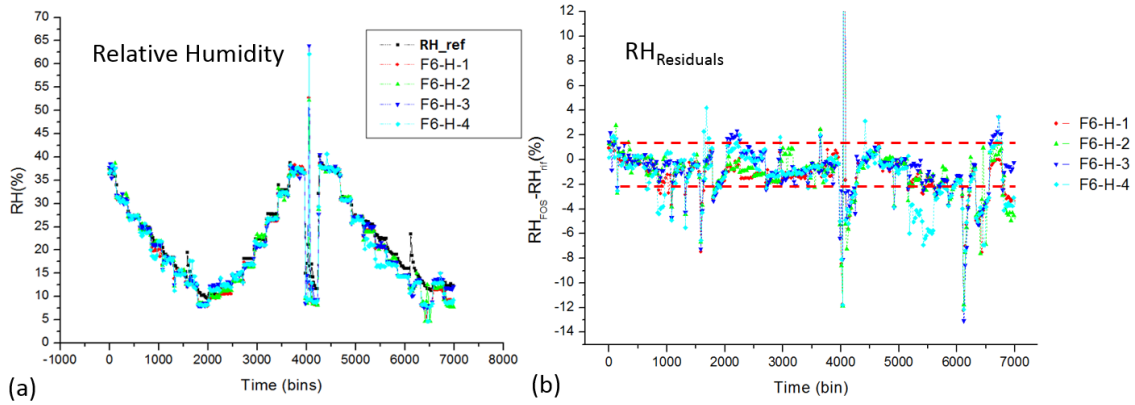


Figure 7. RH measured by a sample of four FOS Thermo-Hygrometer (a) with residuals (b).

5 Radiation hardness study

The radiation processes were performed using a Co^{60} radioactive source. The rad-hard behaviour of the T and RH FOS sensors was studied using sample of sensors.

5.1 Radiation hardness of the FOS temperature sensors

Four samples of Micron Optic T-Sensors from two different batches were irradiated. Six irradiation campaigns were performed, providing to the sensors a total adsorbed dose of 10, 20, 50, 90, 150 and 210 kGy in each intermediate step. The saturation of the radiation-induced wavelength shift and the sensing characteristic of the sensors were investigated.

The T-Sensors were fully characterized before and after each campaign during specific tests at low humidity, changing T typically in the range $[0-20]^{\circ}\text{C}$.

In figure 8a results of the campaigns are summarized, for one of the four tested sensors.

A radiation-induced red shift was observed at each irradiation step, confirming the observation found in literature [9]. In particular, all the four samples show very similar shift values. The S_T values, evaluated as the slope of the calibration curves at each irradiation level, are completely unchanged all over the six campaigns (figure 8b).

As for the observed λ_B shift after each irradiation campaign, it is possible to find a correlation between the radiation-induced wavelength shift ($\Delta\lambda_{ri}$) and the total adsorbed dose (D):

$$\Delta\lambda_{ri} = aD + (bD)/(1 + cD) + d. \quad (5.1)$$

Figure 8c shows the fit with the parameters a , b , c and d . The observed wavelength shift is not saturated up to 210 kGy. However, above 100 kGy total adsorbed dose, the worst case scenario is that the shift continues increasing linearly with the dose. Figure 8d shows the values of the derivative of the dose induced shift, i.e. the sensitivity of the sensor to irradiation ($S_{\gamma,irr}$).

After an adsorbed dose of 150 kGy, $S_{\gamma,irr}$ is found to be below 0.15 pm/kGy for all the tested sensors. From FLUKA simulations it is possible to estimate the dose which approximately will be absorbed by the sensors during their lifetime, according to their location in CMS (e.g. radial distance from the beam pipe) and to the LHC integrated luminosity.

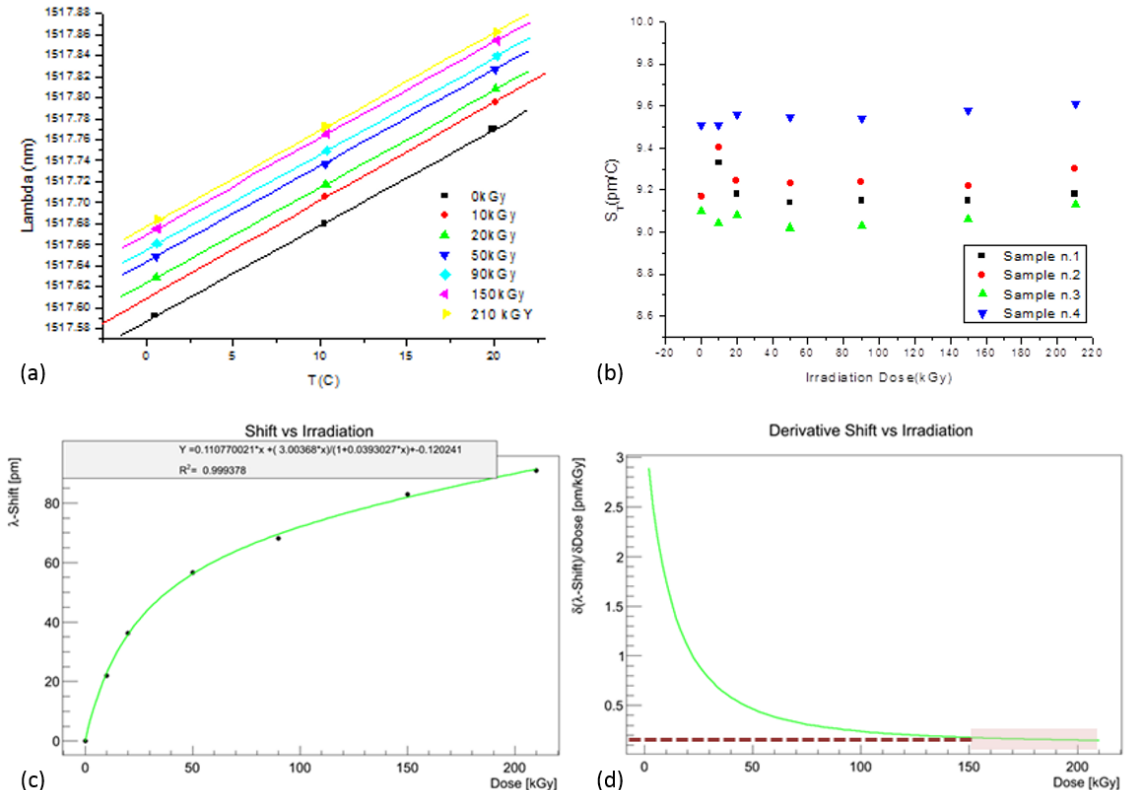


Figure 8. Radiation-induced wavelength shift after each irradiation step (a). S_T independence on radiation dose (b). Radiation-induced wavelength shift as a function of the total adsorbed dose (c). Derivative of the shift vs. irradiation dose (d).

As a matter of fact, the FOS thermo-hygrometers will be installed in the experiment not closer than 400 mm to the beam pipe. This means that, according to the simulations, considering a 150 fb^{-1} integrated luminosity, which corresponds to a three-year long run of the LHC, the estimated absorbed dose of the sensors will be around 12 kGy. This value corresponds to a wavelength shift of 1.8 pm due to irradiation which can be converted into temperature using eq. (4.1). Thus, the estimated radiation induced error in terms of temperature is roughly 0.18°C which is comparable with the temperature measurement accuracy of the sensors (see figure 4b).

The above mentioned results show that we can use this kind of technology in the CMS experiment, just performing a pre-irradiation step of the sensors at a dose higher than 150 kGy in order to bring them in the ‘low γ -radiation sensitivity zone’- taking in account the installation position.

5.2 Radiation hardness of the FOS relative humidity sensors

As the RH-Sensors are polyimide coated FBGs, their response to ionizing radiation may differ from the T-Sensors. To investigate their behaviour, four samples of RH-Sensors from the same batch were irradiated. Three irradiation campaigns were performed, providing to the sensors a total adsorbed dose of 10, 50, 90 kGy in each intermediate. The sensors were characterized after each campaign, performing RH tests at constant T and changing the relative humidity in the range [0–50]%.

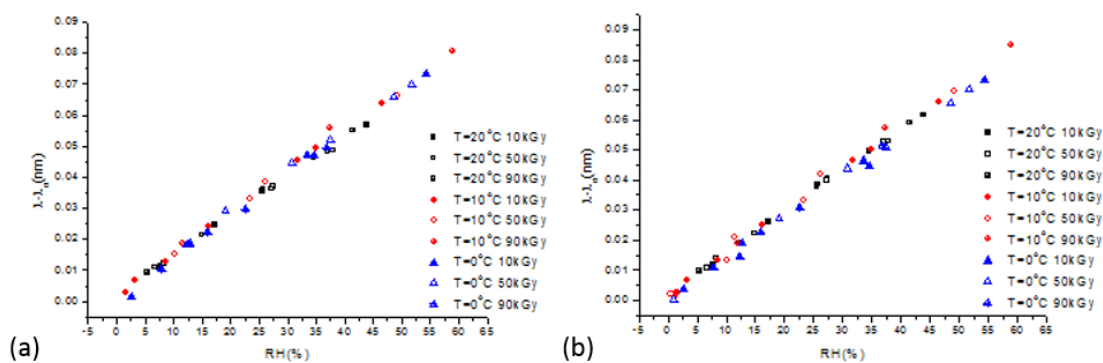


Figure 9. Observed wavelength shift as a function of RH at each irradiation step — two samples (a, b).

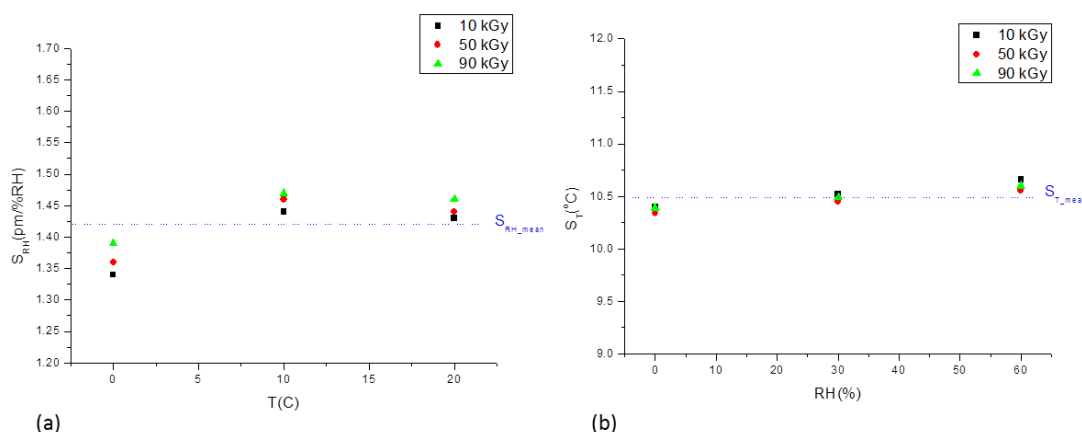


Figure 10. Radiation dependence of S_{RH} (a) and S_T (b).

Figure 9 shows the observed wavelength shifts as a function of the RH for two selected sensors, at each irradiation step. Figure 10 shows the radiation dependence of the S_{RH} and S_T in case of a sample sensor. The mean Relative Humidity Sensitivity S_{RH_mean} was found to be 1.42 pm/%RH with a standard deviation of 0.05 pm/%RH. It was also found that the variation of S_{RH} with the dose at each considered temperature and the variation of S_{RH} with the temperature at each level of radiation are below the mean value error (0.04 pm/%RH and 0.02 pm/%RH respectively). A similar analysis was performed concerning the Temperature Sensitivity of the same sample. In this case, S_{T_mean} was found to be 10.49 pm/°C with a standard deviation of 0.10 pm/°C and the variation of S_T with the dose at three levels of humidity (0, 30 and 60%RH) as well as its variation with RH at each dose were found to be inside the mean value error (0.10 pm/°C and 0.04 pm/°C, respectively). By the way, the T and RH sensitivities variations are inside the measurement error and for this reason can be considered negligible.

Similarly to the T-Sensors, the RH-Sensors also show radiation induced wavelength shift. Also in this case, preliminary observations suggest that a pre-irradiation step helps decreasing the sensitivity to further radiation. Progressive irradiation campaigns are on-going to define the saturation properties.

6 Conclusions

In this work we presented the results obtained by extensive testing campaigns of optical thermohygrometers based on Fiber Bragg Grating, carried out in the PH-DT laboratory of CERN. The temperature and relative humidity sensors were fully characterized in the temperature range $[-20-20]^{\circ}\text{C}$ and also after exposition to strong γ -ionizing radiation. The results showed that the sensing performances are completely unaffected by the incremental absorbed dose, while the natural wavelength peak of each sensor exhibits a radiation-induced shift, which has to be taken into account. Collected results give a clear demonstration that this innovative technology is a robust and valid alternative to currently used polymer-based electronic hygrometers in the CMS experiment. For these reasons it has been selected for hygrometric control of the air in critical areas of the experiment, where cold services are exposed to risk of condensation.

References

- [1] F. Berghmans and A. Gusarov, *Fiber bragg grating sensors in nuclear environments*, in *Fiber Bragg Grating Sensors: Recent Advancements, Industrial Applications and Market Exploitation*, A. Cusano, A. Cutolo and J. Albert eds., Bentham Science Publishers, (2011), pg. 218–237.
- [2] Z. Szillási et al., *One Year of FOS Measurements in CMS Experiment at CERN*, *Physics Procedia* **37** (2012) 79.
- [3] P. Kronenberg, P.K. Rastogi, P. Giaccari and H.G. Limberger, *Relative humidity sensor with optical fiber Bragg gratings*, *Opt. Lett.* **26** (2002) 1375.
- [4] T.L. Yeo, T. Sun, K.T.V. Grattan, D. Parry, R. Lade and B.D. Powell, *Polymer-Coated Fiber Bragg Grating for Relative Humidity Sensing*, *IEEE Sens. J.* **5** (2005) 1082.
- [5] G. Berruti et al., *Radiation hard humidity sensors for high energy physics applications using polyimide-coated Fiber Bragg Gratings sensors*, *Sensor. Actuator. B* **177** (2013) 94.
- [6] M.A. Caponero et al., *Monitoring relative humidity in RPC detectors by use of fiber optic sensors*, 2013 *JINST* **8** T03003.
- [7] K.O. Hill and G. Meltz, *Fiber Bragg Grating Technology Fundamentals and Overview*, *J. Lightwave Technol.* **15** (1997) 1263.
- [8] T.L. Yeo, T. Sun, K.T.V. Grattan, D. Parry, R. Lade and B.D. Powell, *Characterization of a polymer-coated fibre Bragg grating sensor for relative humidity sensing*, *Sensor. Actuator. B* **110** (2005) 148.
- [9] A. Gusarov et al., *High total dose radiation effects on temperature sensing fiber bragg gratings*, *IEEE Photon. Tech. Lett.* **11** (1999) 1159.